CHAPTER 8

Computational Investigation on the MDM2-Idasanutlin Interaction Using the Potential of Mean Force Method

Computational Investigation on the MDM2-Idasanutlin Interaction Using the Potential of Mean Force Method

8.1. Abstract:

The MDM2 protein is a well-studied primary negative regulator of the tumor suppressor p53 molecule. Therefore, nowadays many research studies have focused on the inhibition of MDM2 with potent inhibitors. Idasanutlin (RG7388) is a well-studied small molecule, the antagonist of MDM2 with potential antineoplastic activity. Nevertheless, the highly significant information pertaining to the free energy profile, intermediates, and the association of receptor and ligand components in the MDM2-idasanutlin complex remains unclear. Here we have studied the free energy profile of the MDM2-idasanutlin complex in terms of the PMF method. We have used the PMF method coupled with US simulations to generate the free energy profile for the association of NTD of MDM2 and idasanutlin along with a specific reaction coordinate for identifying transition states, intermediates as well as the relative stabilities of the endpoints. We also have determined the binding characteristics and interacting residues at the interface of the MDM2-idasanutlin complex from the BFE and PRED analyses. The PMF minima for the MDM2-idasanutlin complex was observed at a center of mass (CoM) distance of separation of 11 Å with dissociation energy of 17.5 kcal mol^{-1}. As a function of the distance of separation of MDM2 from idasanutlin, we also studied the conformational dynamics as well as stability of the NTD of MDM2. We found that there is indeed a high binding affinity between MDM2 and idasanutlin ($\Delta G_{binding}$ = -3.19 kcal mol^{-1}). We found that in MDM2, the residues MET54, VAL67, and LEU58 provide the highest energy input for the interaction between MDM2 and idasanutlin.

8.2. Introduction:

p53 is a tumour suppressor protein made of 393 amino acids. It also acts as a transcription factor, which trans-activates a number of genes in response to different forms of genotoxic stress by binding to particular DNA sequences, thus halting the cell cycle, restoring damaged DNA, or inducing apoptosis as the cell fates [651, 652]. The structure of the p53 core DNA-binding domain (residues 94-312) binding directly to the DNA sequence was resolved by X-ray crystallography. Both X-ray crystallography and

NMR analyses were used to deduce the structure of the tetramerization domain (residues 323–356) of the p53 protein [653-655]. Trans-activity of p53 is regulated either by post-translation mechanisms such as acetylation, phosphorylation, and isomerization of prolyls, or by Protein-Protein Interaction (PPI) [656-661]. p53 can pick a subset of target promoters through these mechanisms, by modifying its structure as well as the affinity to bind to the DNA sequences containing variations within the downstream genes. However, the mechanism responsible for downstream gene selectivity and the subsequent cell fate remains unclear [662]. MDM2 is a well-studied negative regulator of p53. The N Terminal Domain (NTD) of MDM2 is the primary site of interaction for p53. There exists a mutual regulation between p53 and MDM2 maintained *via* a feedback loop, by which a balance of the two molecules are maintained in cells [663-671].

The RG7388 (idasanutlin) molecule is a second-generation potent MDM2 inhibitor. It binds to the p53 binding site present in the NTD of MDM2. It was developed with the goal to improve the conformational and stereochemical properties of the molecules comprised in the spirooxindole series by instigating the cyanopyrrolidine core, which was assumed to possess more flexibility [672]. This molecule was found to exhibit more potency, more selectivity, and an enhanced pharmacokinetic (PK) profile when compared to another potent MDM2 inhibitor, RG7112 [673, 674]. RG7388 was also found to exhibit dose-dependent p53 stabilization, cell cycle arrest, and apoptosis.

In the recent study, the photo activation of a photoactivatable MDM2 inhibitor, idasanutlin, bound to a Photoremovable Protecting Group (PPG) to disrupt the p53-MDM2 interaction was demonstrated. In that study, Idasanutlin was found not to hinder the p53-MDM2 interaction when it was bound to a PPG. However, when the PPG-idasanutlin complex was photo-irradiated (400 nm irradiation), the active inhibitor idasanutlin that was released from the PPG-idasanutlin complex, blocks the p53-MDM2 interaction, leading to either senescence or cell death. But the mechanism of idasanutlin inhibition of p53-MDM2 interaction is not understood well. So it is necessary to understand the binding characteristics of idasanutlin with the NTD of MDM2.

In the present study, we have determined the association and the free energy profile of the MDM2-idasanutlin complex in terms of the PMF. We have also investigated the conformational dynamics and stability of MDM2 as a function of its center of mass (CoM) distance from idasanutlin. We also carried out BFE and PRED analyses to infer the binding characteristics and identify hotspot residues across the interface of the MDM2-

idasanutlin complex.

8.3. Materials & Methods:

Using the RMSD clustering algorithm, the lowest energy conformer of the MDM2-idasanutlin complex was extracted from the 40 ns Molecular Dynamics (MD) simulation trajectory obtained from our previous study [675]. The lowest energy conformer so obtained was taken as the initial complex structure of MDM2-idasanutlin in this PMF study. The distance between MDM2 and idasanutlin in this complex structure was calculated prior to the PMF study and was found to be 12 Å.

8.3.1. PMF Calculation:

The PMF of the MDM2-idasanutlin complex has been calculated implying the equilibrium US simulations by the means of the WHAM. The rest of the steps have been performed as mentioned in section **4.3.3**, where the distance between CoMs of the MDM2 and idasanutlin molecules was changed with time from 6 Å to 26 Å spanning different configurations.

8.3.2. RMSD and Intramolecular hydrogen bond analyses for MDM2 as a function of CoM distance from Idasanutlin:

Using the Visual Molecular Dynamics (VMD) package, the generated trajectories were visualized after each MD run. Using the centering and standard deviation process, the PMF data were normalized at a broad separation of MDM2 and idasanutlin in the system. For MDM2 and MDM2-idasanutlin complexes, RMSD and intermolecular hydrogen bond analysis were performed only for all the increasing and decreasing coordinates, respectively. RMSD was calculated using the MDM2-idasanutlin complex with the centre of the mass distance of separation of 12 Å (the initial structure) as a reference structure.

8.3.3. BFE and PRED of the MDM2-idasanutlin Complex:

In this work, the relative BFE and PRED of the MDM2-idasanutlin complex interface residues were determined using the procedure mentioned in section **4.3.6.**

8.4. Results & Discussions:

8.4.1. PMF profile of MDM2-idasanutlin complex:

The lowest energy conformer of the MDM2-idasanutlin complex with the center of a mass distance of 12 Å was taken as the initial complex structure for the PMF study [676-682]. The PMF analysis for the MDM2-idasanutlin complex was carried out in the water at room temperature, and the PMF profile obtained has been plotted as a function of reaction coordinate (**Figure 8.1**). The reaction coordinate has been defined as the distance of separation between the CoMs of MDM2 and idasanutlin. From **Figure 8.1**, a minimum PMF value of the MDM2-idasanutlin complex was observed at a distance of separation of 11 Å. The dissociation energy value of the complex was found to be 17.5 kcal mol^{-1}. We found no interaction between MDM2 and idasanutlin when they are separated by a CoM distance of 20 Å and above. But when the CoM distance of separation between MDM2 and idasanutlin is gradually decreased from the optimum distance of 11 Å, the dissociation energy has been witnessed to increase due to the existence of strong van der Waals repulsion between MDM2 and idasanutlin.

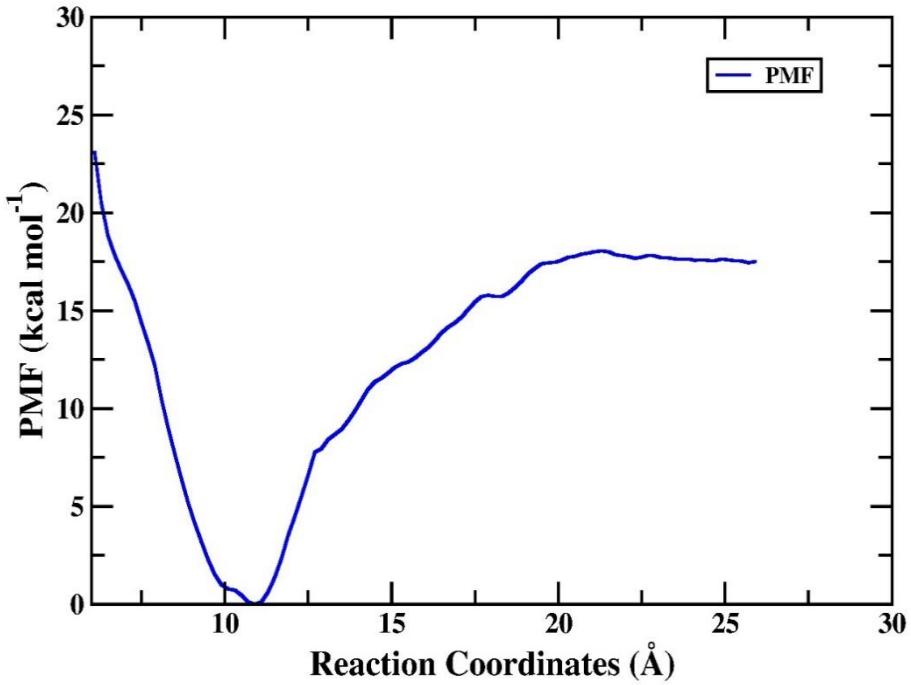

Figure 8.1. *Potential of Mean Force as a function of the reaction coordinate for the association and dissociation of the MDM2-Idasanutlin complex.*

8.4.2. Determination of the interface interactions of the p53(TAD1)-MDM2(NTD) Complex:

The MDM2-idasanutlin complex structure with a CoM distance of separation of 11 Å was extracted (**Figure 8.2a**) based on the PMF value from the free energy profile. The 3-D complex structure was then submitted to the PDBsum server and the protein ligand interaction profile (**Figure 8.3 and Table 8.1**) was obtained. **Figure 8.3** shows the LigPlot analysis for the complex structure obtained from PDBsum server. From **Table 8.1**, we can see the MDM2-idasanutlin complex structure was stabilized by one hydrogen bond and thirty-four non-bonded contacts.

8.4.3. Secondary Structure comparison of the MDM2-idasanutlin Complex with the p53(TAD1)-MDM2(NTD) complex (PDB ID:1YCR):

On the other hand, the complex structure was superimposed with the 3D structure of p53 bound to the NTD of MDM2 (PDB ID: 1YCR) (**Figure 8.2b**). The RMSD between the MDM2-idasanutlin complex and the p53-MDM2 complex has been found to be 1.035 Å. In addition, the secondary structure content of MDM2 present in the MDM2-idasanutlin complex and the p53-MDM2 complex have been calculated using the 2StrucCompare server (**Table 8.2**) [678], it was found that MDM2 present in the MDM2-idasanutlin complex has 47% helices and 10% sheets while MDM2 present in the p53-MDM2 complex has 35% helices and 13% sheets.

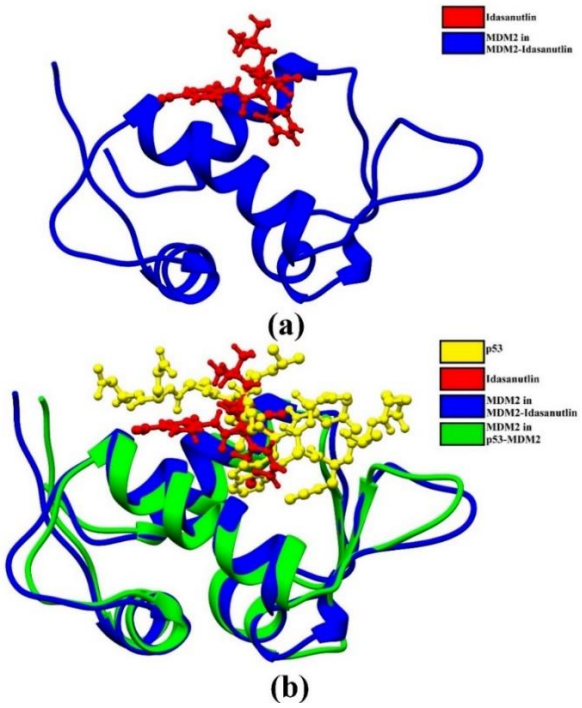

Figure 8.2. *(a) 3D structure of MDM2-idasanutlin complex with center of mass distance of separation of 11 Å (b) 3D structure of MDM2-idasanutlin complex with center of mass distance of separation of 11 Å superimposed with the 3D structure of p53 bound to the NTD of MDM2 (PDB ID: 1YCR).*

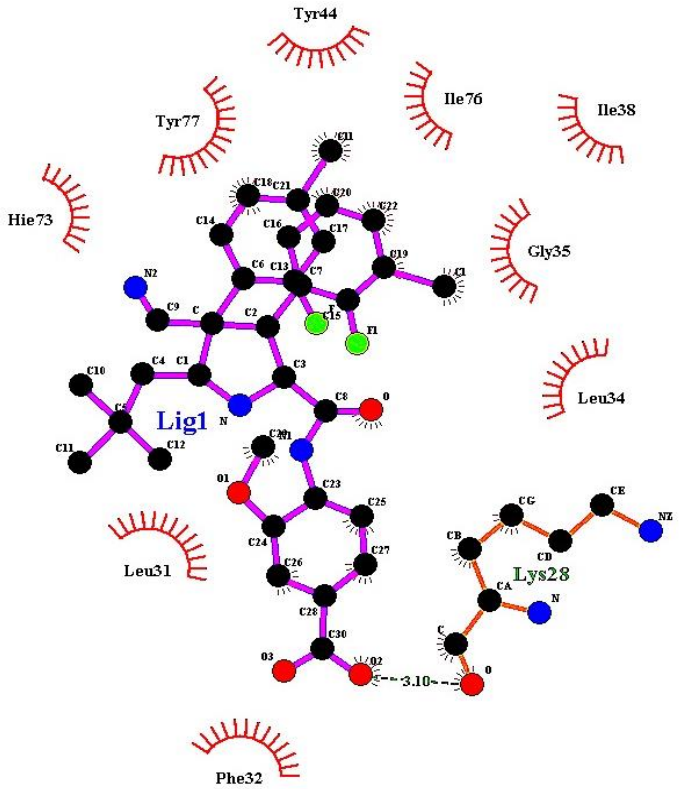

Figure 8.3. *Protein-Ligand Interaction profile of MDM2-Idasanutlin complex with PMF minima.*

Table 8.1. *Protein-Ligand interaction profile of the MDM2-idasanutlin complex with centre of mass distance of separation of 11 Å.*

List of protein-ligand interactions											
Hydrogen bonds											
	Atom 1					Atom 2					
	Atom No.	Atom Name	Res. Name	Res. No.	Chain	Atom No.	Atom Name	Res. Name	Res. No.	Chain	Dist.
1.	534	O	LYS	28	M	7	O2	LIG	1	M	3.10
Non-bonded contacts											
	Atom 1					Atom 2					
	Atom No.	Atom Name	Res. Name	Res. No.	Chain	Atom No.	Atom Name	Res. Name	Res. No.	Chain	Dist.
1.	639	CD2	LEU	34	M	1	Cl	LIG	1	M	3.79
2.	645	N	GLY	35	M	1	Cl	LIG	1	M	3.73
3.	647	CA	GLY	35	M	1	Cl	LIG	1	M	3.88
4.	703	CD1	ILE	38	M	1	Cl	LIG	1	M	3.68
5.	1262	CB	HIE	73	M	2	C11	LIG	1	M	3.74
6.	1274	O	HIE	73	M	2	C11	LIG	1	M	3.35
7.	1325	CB	ILE	76	M	2	C11	LIG	1	M	3.71
8.	1357	CD2	TYR	77	M	2	C11	LIG	1	M	3.77
9.	1355	CE2	TYR	77	M	2	C11	LIG	1	M	3.40
10.	1352	CZ	TYR	77	M	2	C11	LIG	1	M	3.42
11.	1353	OH	TYR	77	M	2	C11	LIG	1	M	3.86
12.	1211	CG1	VAL	70	M	3	F	LIG	1	M	3.00
13.	584	O	LEU	31	M	4	F1	LIG	1	M	3.08
14.	593	CD1	PHE	32	M	5	O	LIG	1	M	3.75
15.	533	C	LYS	28	M	7	O2	LIG	1	M	3.67
16.	534	O	LYS	28	M	7	O2	LIG	1	M	3.10
17.	517	CB	LYS	28	M	7	O2	LIG	1	M	3.75
18.	520	CG	LYS	28	M	7	O2	LIG	1	M	3.81
19.	579	CD2	LEU	31	M	30	C18	LIG	1	M	3.70
20.	1352	CZ	TYR	77	M	30	C18	LIG	1	M	3.76
21.	1353	OH	TYR	77	M	30	C18	LIG	1	M	3.38
22.	647	CA	GLY	35	M	31	C19	LIG	1	M	3.63
23.	818	OH	TYR	44	M	32	C20	LIG	1	M	3.40
24.	647	CA	GLY	35	M	34	C22	LIG	1	M	3.52
25.	818	OH	TTYR	44	M	34	C22	LIG	1	M	3.67
26.	593	CD1	PHE	32	M	37	C25	LIG	1	M	3.33
27.	534	O	LYS	28	M	38	C26	LIG	1	M	3.34
28.	593	CD1	PHE	32	M	39	C27	LIG	1	M	3.49
29.	583	C	LEU	31	M	41	C29	LIG	1	M	3.79
30.	584	O	LEU	31	M	41	C29	LIG	1	M	3.89
31.	570	CB	LEU	31	M	41	C29	LIG	1	M	3.78
32.	573	CG	LEU	31	M	41	C29	LIG	1	M	3.77

33.	579	CD2	LEU	31	M	41	C29	LIG	1	M	3.65
34.	585	N	PHE	32	M	41	C29	LIG	1	M	3.89
Number of hydrogen bonds: 1											
Number of non-bonded contacts: 34											

Table 8.2. *Secondary structure analysis of the lowest energy structure of MDM2-Idasanutlin complex and p53-MDM2 complex (PDB ID: 1YCR) using 2Struc online server.*

	α-Helix (%)	**3_{10}-Helix (%)**	**Turns (%)**
MDM2-Idasanutlin	42.4	3.5	12.9
p53-MDM2	34.9	0	11.9

8.4.4. Analysis of conformational dynamics of MDM2(NTD) as a function of its CoM distance from idasanutlin:

Throughout the US simulation of the MDM2-idasanutlin complex, the MDM2 molecule was found to undergo rapid conformational changes. The snapshots of the MDM2-idasanutlin complex at different windows of the distance of separation were generated using University of California, San Francisco (UCSF) Chimera v.1.13.1 (**Figure 8.4**).

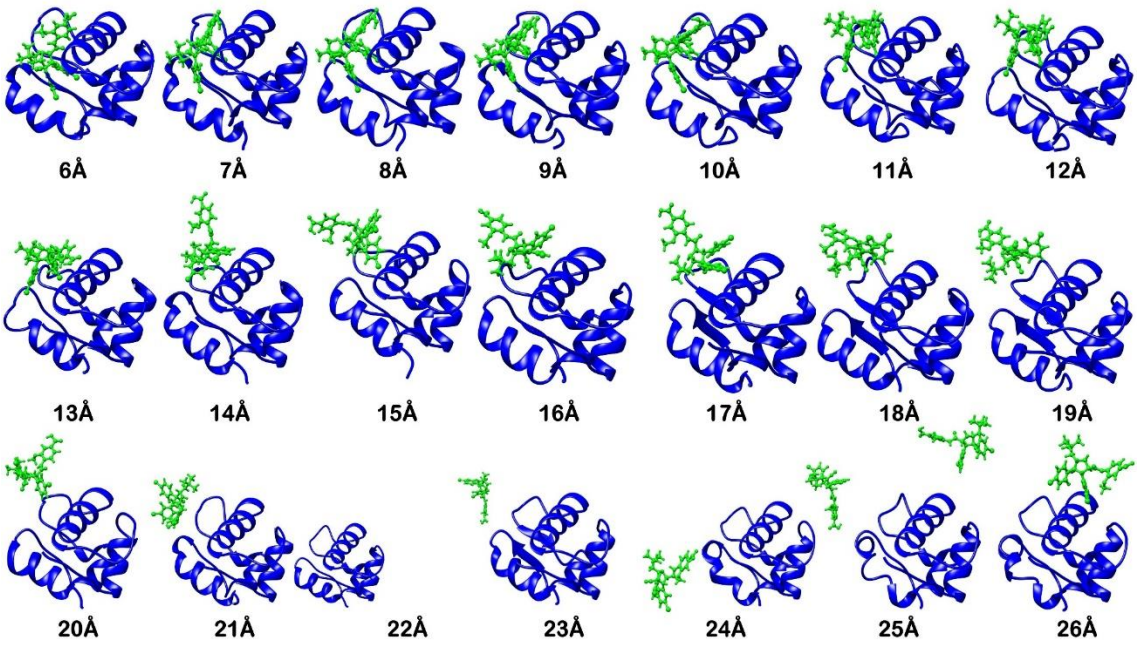

Figure 8.4. *Snapshots of MDM2-Idasanutlin complex structures when idasanutlin is at discrete distance of separation (in Å) from MDM2.*

8.4.5. RMSD analysis for MDM2(NTD) as a function of its CoM distance from idasanutlin:

Then the RMSD analysis has been carried out to investigate the structural stability of NTD of MDM2 in the MDM2-idasanutlin complex during the course of US simulation. (**Figure 8.5a**) represents the RMSD profile for the MDM2 protein in the MDM2-idasanutlin complex when the CoM distance of separation between MDM2 and idasanutlin is shifted from 12 Å to 6 Å. (**Figure 8.5b**) represents the RMSD profile for the MDM2 protein in the MDM2-idasanutlin complex when the CoM distance of separation between MDM2 and idasanutlin is shifted from 12 Å to 26 Å. From (**Figure 8.5a**), we notice MDM2 to undergo conformational changes more rapidly when idasanutlin approaches closer to MDM2 from 12 Å. This happens because of an upsurge in the strong van der Waals forces with a gradual decrease in the distance of separation between MDM2 and idasanutlin. From (**Figure 8.5b**), the MDM2 molecule has been found to hold various folding at different distance intervals (from 12 Å to 26 Å) of idasanutlin from MDM2. It can be seen that MDM2 initially takes a fold at 14 Å, which is maintained until MDM2 and idasanutlin are separated by a distance of 24 Å. When the distance of separation between MDM2 and idasanutlin exceeds 24 Å, no further interactions can be seen between MDM2 and idasanutlin, which results in rapid conformational changes in MDM2. Overall from the RMSD analysis, it can be seen that when idasanutlin is at an equilibrium distance of 11-12 Å from MDM2, the structure of NTD of MDM2 was found to be quite stable than at the other distances of separation.

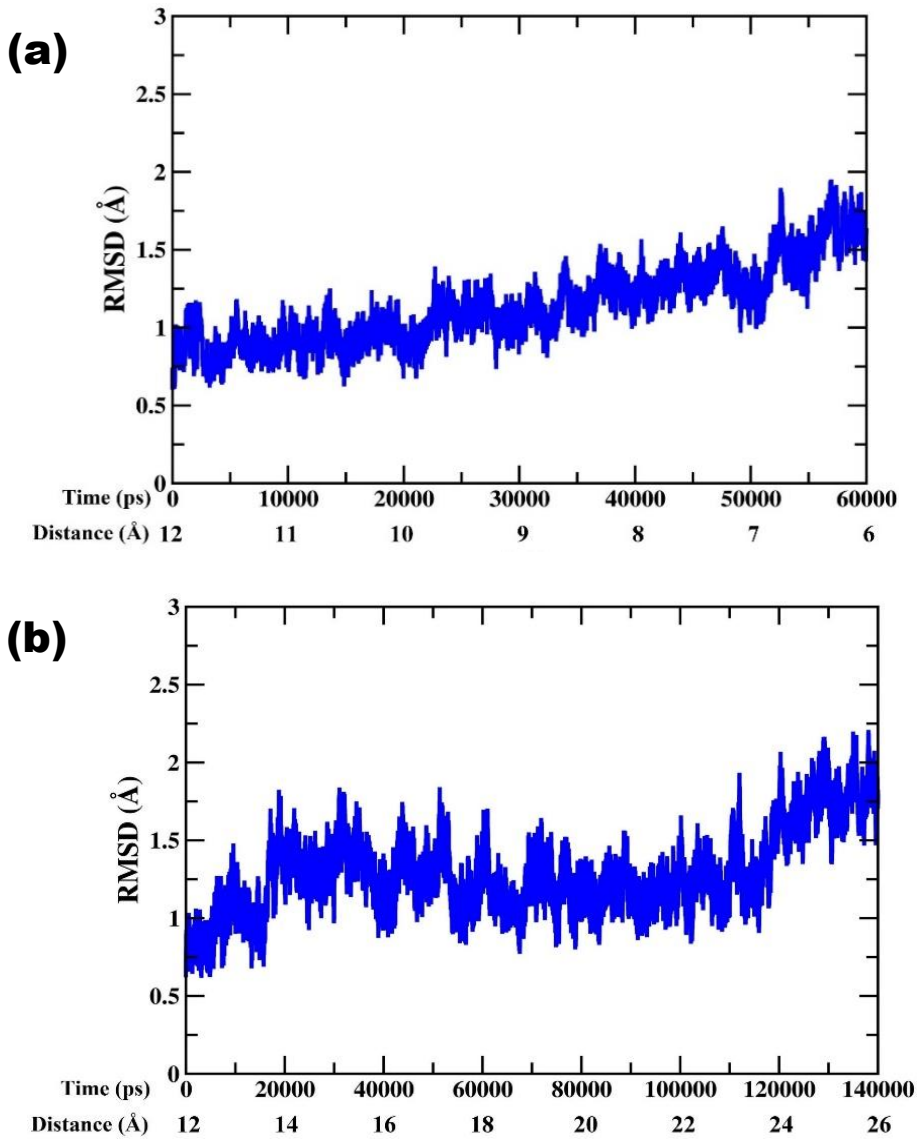

Figure 8.5. *RMSD analysis for MDM2 when the distance of separation between MDM2 and idasanutlin shifted (a) from 12 Å to 6 Å; and (b) from 12 Å to 26 Å.*

8.4.6. Intramolecular hydrogen bond analysis for MDM2(NTD) as a function of its CoM distance from idasanutlin:

The intermolecular hydrogen bond analysis for the MDM2-idasanutlin complex has been carried out by utilizing the trajectory files created from each window throughout the PMF analysis. The intermolecular hydrogen bond profiles for the MDM2-idasanutlin complex have been depicted as a function of the CoM distance of separation between MDM2 and Idasanutlin. From **Figure 8.6a** and **8.6b**, it can be observed that the number of intermolecular hydrogen bonds present in the MDM2-idasanutlin complex to increase

markedly when the CoM distance of separation between MDM2 and idasanutlin increases or decreases from 12 Å. This happens because the binding affinity between MDM2 and idasanutlin varies as a function of the distance of separation between them.

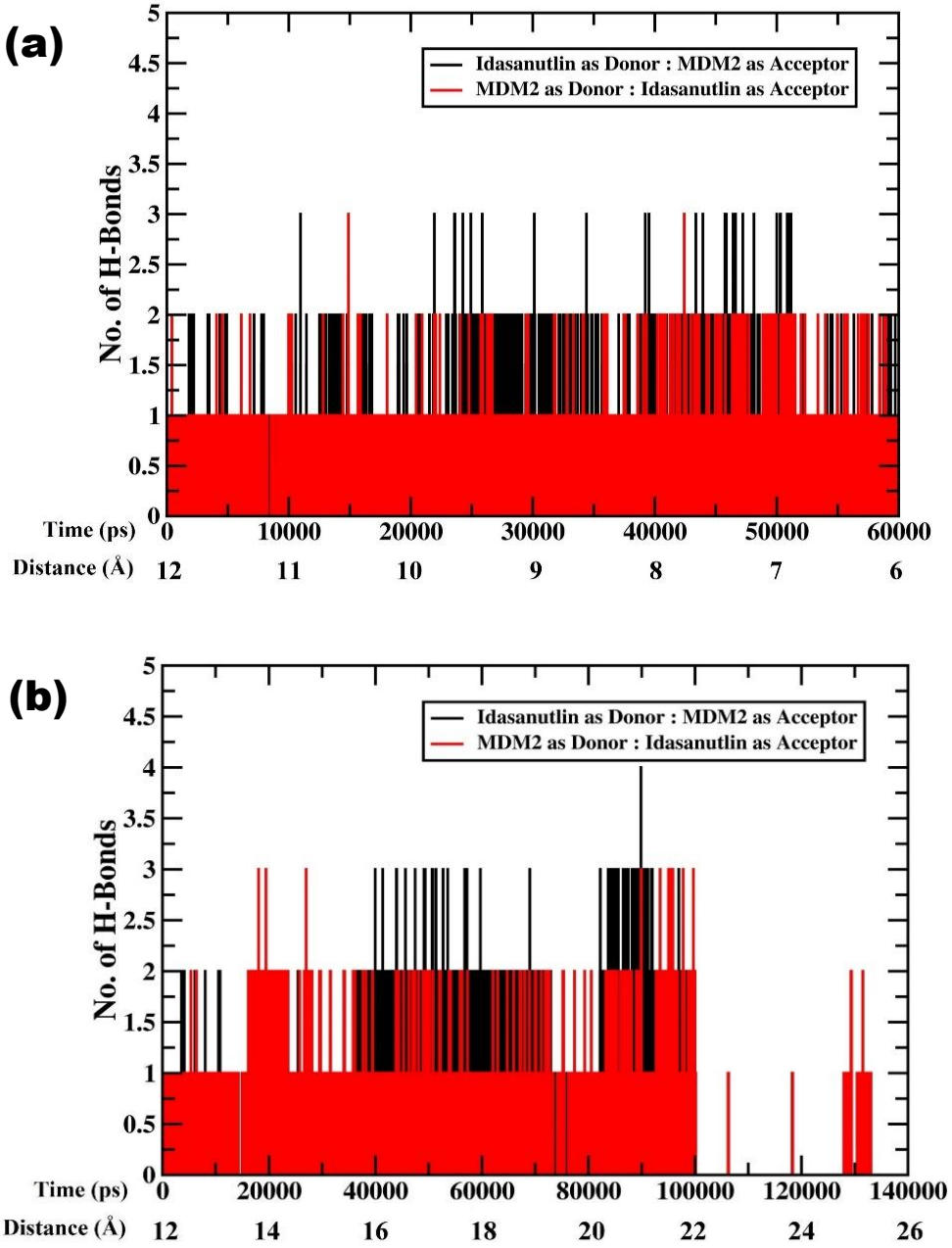

Figure 8.6. *Inter-molecular hydrogen bond analysis for MDM2 when the distance of separation between MDM2 and idasanutlin shifted (a) from 12 Å to 6 Å; and (b) from 12 Å to 26 Å.*

8.4.7. BFE and PRED analyses of the MDM2-idasanutlin complex:

The BFE calculations of MDM2 and idasanutlin to form the MDM2-idasanutlin complex were performed using the MM-PBSA method [683-690], a module of the AMBER14 software package. For the BFE and PRED analysis, we have used the 10 ns MD trajectory obtained from the production dynamics of the MDM2-idasanutlin complex with the center of the mass distance of separation of 11 Å. The BFE evaluated for the MDM2-idasanutlin complex, together with the descriptions of the energy terms, are shown in Table **8.3**.

Table 8.3. *The various components of the BFE (kcal mol^{-1}) evaluated by MM/PBSA method between MDM2 and idasanutlin in the MDM2-Idasanutlin complex.*

Components	**Complex (kcal mol^{-1})**	**Standard Deviation (±)**	**Receptor (kcal mol^{-1})**	**Standard Deviation (±)**	**Ligand (kcal mol^{-1})**	**Standard Deviation (±)**	**$\Delta\Delta G_{bind}$ (kcal mol^{-1})**	**Standard Deviation (±)**
$\Delta E_{VDWAALS}$	-673.14	11.05	-628.54	10.28	-7.27	1.86	-37.33	2.67
ΔE_{EL}	-6024.41	46.17	-5938.92	44.09	-81.76	3.31	-3.72	3.87
ΔE_{PB}	-1228.84	26.36	-1209.91	25.74	-36.26	1.65	17.33	2.96
ΔE_{NPOLAR}	803.07	3.96	773.14	4.05	59.53	0.39	-29.59	1.51
ΔE_{DISPER}	-510.59	4.64	-506.38	4.55	-54.86	0.38	50.65	1.63
ΔG_{gas}	-6697.54	43.05	-6567.46	40.56	-89.04	3.57	-41.05	4.60
ΔG_{solv}	-936.37	24.07	-943.16	24.01	-31.59	1.58	38.38	2.69
ΔG_{TOTAL}	-7633.91	27.06	-7510.61	24.64	-120.62	3.01	**-2.67**	3.43
TS_{TRA}	15.98	0	15.93	0	13.45	0	-13.40	0
TS_{ROT}	15.81	0	15.76	0.01	11.55	0	-11.50	0.01
TS_{VIB}	1052.95	1.41	980.75	1.22	46.78	0.012	25.42	1.44
TS_{TOT}	1084.74	1.41	1032.43	1.22	71.78	0.012	**0.52**	1.44
$\Delta G_{binding}$							**-3.19**	

ΔE_{EL} = electrostatic energy as calculated by the MM force field; **$\Delta E_{VDWAALS}$** = van der Waals contribution from MM; **ΔE_{PB}** = the electrostatic contribution to the polar solvation free energy calculated by PB; **ΔE_{NPOLAR}** = non-polar contribution to the solvation free energy calculated by an empirical model; **ΔG_{gas}** = total gas phase energy (**$\Delta G_{gas} = \Delta E_{EL} + \Delta E_{VDWAALS}$**); **$\Delta G_{solv}$** = sum of nonpolar and polar contributions to solvation; **$\Delta G_{GB\_TOT}/\Delta G_{PB\_TOT}$** = final estimated binding free energy in kcal mol^{-1} calculated from the terms above (**$\Delta G_{TOTAL} = \Delta G_{gas} + \Delta G_{solv}$**). translational energy (**TS_{TRA}**); rotational energy (**TS_{ROT}**); vibrational energy (**TS_{VIB}**), total entropic contribution (**TS_{TOT}**); and BFE (**$\Delta G_{binding}$**).

From Table **8.3**, all the derived components required for the BFE analysis have been observed to contribute to the binding of MDM2 and idasanutlin to form the MDM2-idasanutlin complex. From Table **8.3**, it can be observed that the mean TS_{VIB} is higher than TS_{ROT} and TS_{TRA} in the complex, receptor, and ligand as the vibration in molecules

between their atoms occurs at a rate usually much more frequent than rotational and translational ones.

The $\Delta G_{binding}$ value for the MDM2-idasanutlin complex was found to be -3.19 kcal mol^{-1}. This value is quite near to -7.29 kcal mol^{-1}, which is the $\Delta G_{binding}$ value for the p53-MDM2 complex calculated using the MM-PBSA method [679].

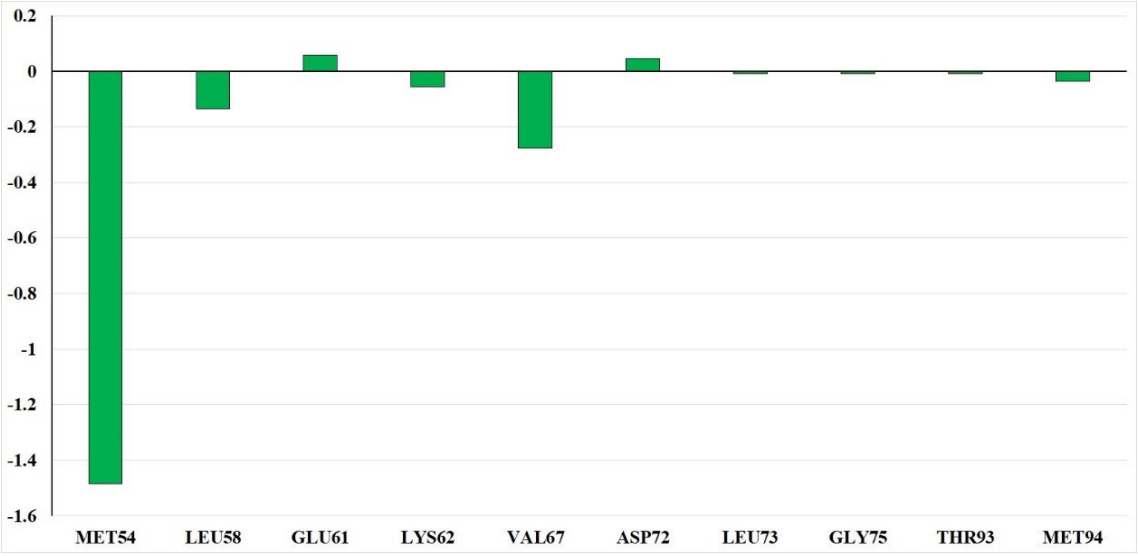

Figure 8.7. *PRED analysis of MDM2 in MDM2(NTD)-Idasanutlin complex.*

8.5. Conclusion:

In this study, we have demonstrated the free energy profile and the association of the MDM2-idasanutlin complex along with a specific reaction coordinate using the PMF. The MDM2-idasanutlin complex structure with optimal energy was noticed at 11 Å separation and the dissociation energy of the complex was found to be 17.5 kcal mol^{-1}. We also see the effect of the CoM distance of separation between MDM2 and idasanutlin on the stability of the MDM2 molecules. The binding affinity between MDM2 and idasanutlin was found to be quite high ($\Delta G_{binding}$ = -3.19 kcal mol^{-1}). From the PRED study, we observed the residues MET54, VAL67, and LEU58 of MDM2 provide the highest energy contributions for the interaction between MDM2 and idasanutlin. Our results in this study provide insights into the complex's association/dissociation pathway and the degree of interaction between MDM2 and idasanutlin. These results may be useful in developing potential MDM2 inhibitors that block the interactions between p53 and MDM2.